

A proteomic approach for the discovery of protease substrates

Andrew J. Bredemeyer*, Renate M. Lewis†, James P. Malone†, Alan E. Davis†, Julia Gross†, R. Reid Townsend††, and Timothy J. Ley*[§]

Department of Medicine, Divisions of *Oncology and †Metabolism, Siteman Cancer Center and Proteomics Center, Washington University School of Medicine, St. Louis, MO 63110

Edited by Robert M. Stroud, University of California, San Francisco, CA, and approved June 23, 2004 (received for review April 2, 2004)

Standardized, comprehensive platforms for the discovery of protease substrates have been extremely difficult to create. Screens for protease specificity are now frequently based on the cleavage patterns of peptide substrates, which contain small recognition motifs that are required for the cleavage of the scissile bond within an active site. However, these studies do not identify *in vivo* substrates, nor can they lead to the definition of the macromolecular features that account for the biological specificity of proteases. To use properly folded proteins in a proteomic screen for protease substrates, we used 2D difference gel electrophoresis and tandem MS to identify substrates of an apoptosis-inducing protease, granzyme B. We confirmed the cleavage of procaspase-3, one of the key substrates of this enzyme, and identified several substrates that were previously unknown, as well as the cleavage site for one of these substrates. We were also able to observe the kinetics of substrate cleavage and cleavage product accumulation by using the 2D difference gel electrophoresis methodology. "Protease proteomics" may therefore represent an important tool for the discovery of the native substrates of a variety of proteases.

The detailed investigation of blood coagulation over the past 40 years has become a foundation for the discovery of other intricate proteolytic processing cascades that are now recognized to play major roles in regulating many basic cellular processes (reviewed in ref. 1). A bioinformatics survey of the human genome identified ≈ 500 proteases (2) with 461 listed in the comprehensive MEROPS database (3). The exquisite substrate specificity of "regulatory" proteases is now understood in terms of 3D recognition regions remote to the catalytic domains (exosites) (4).

Although the screening of peptide substrate libraries for protease cleavages can identify consensus recognition motifs in proximity to the active site (5, 6) and aid in the discovery of protease substrates and inhibitors, biological specificities depend on complex interactions between the protease and its folded targets (6). Although many global approaches have been suggested for the study of protease functions (reviewed in ref. 7), 2D gel electrophoresis, in conjunction with tandem MS, is one technique that can potentially identify and characterize natural macromolecular substrates and their products.

We chose the serine protease granzyme (Gzm) B as a test enzyme to evaluate this approach. Gzm B is released from the granules of cytotoxic lymphocytes and induces apoptotic death in target cells by cleaving intracellular proteins. Known substrates include procaspases-3 and -8, Bid, and downstream caspase targets such as the inhibitor of caspase-activated DNase (ICAD) (8). Gzm B-dependent membrane disruption is observed in enucleated cells (9), however, and recent evidence indicates that unidentified substrates of Gzm B may also contribute to mitochondrial changes seen upon Gzm B treatment (10–12). Additionally, cells that are genetically deficient for known substrates [procaspase-3 (13), Bid (12), and ICAD (13, 14)] remain susceptible to Gzm B-induced death, supporting the idea that alternative pathways and/or substrates may be involved. The existence of several well defined targets and the clear potential for additional unrecognized substrates made Gzm B an attractive protease for the exploration of this discovery system.

In this study, we analyzed a large population of murine cellular proteins ($\approx 2,500$ forms) for cleavage by murine Gzm B using 2D difference gel electrophoresis (2D DIGE) (15, 16) and tandem MS. We report the identification of several natural substrates and the time-dependent appearance and characterization of macromolecular products.

Materials and Methods

Gzm Treatment of YAC-1 Cell Lysates. YAC-1 cells (mouse lymphoma) were washed in PBS and resuspended at 10^8 cells per ml in 25 mM Tris-HCl/30 mM NaCl/1 mM DTT, pH 8.0, containing the caspase inhibitors *N*-benzyloxycarbonyl-Asp-Glu-Val-Asp fluoromethylketone (z-DEVD-fmk) and benzyloxycarbonyl-Val-Ala-Asp-fluoromethyl ketone (z-VAD-fmk) (100 μ M each; Calbiochem) or vehicle control (DMSO). Cells were incubated with the inhibitors for 15 min at 37°C and then subjected to three rounds of freeze/thaw lysis. Lysates were cleared by centrifugation and treated with 1 μ M recombinant Gzm A (rGzm A) (17), 1 μ M rGzm B (18), rGzm B preincubated with the Gzm B inhibitor acetyl-Ile-Glu-Thr-Asp-CHO (Ac-IETD-CHO) (200 μ M; Calbiochem), or vehicle only, at 37°C. All samples were then solubilized in three volumes of lysis buffer {7 M urea/2 M thiourea/4% 3-[(3-cholamidopropyl)dimethylammonio]-1-propanesulfonate (CHAPS)/30 mM Tris-HCl, pH 8.5}.

Western Blot Analysis and *in Vitro* Cleavage Assay. Before solubilization of lysates for 2D DIGE, aliquots were removed and were analyzed by Western blotting. Rabbit anti-caspase 3 (AAP-103, Stressgen Biotechnologies, Victoria, Canada) was used at 1:1,000, goat anti-Bid (AF 860, R & D Systems) at 1:1,000, and rabbit anti-ICAD (550736, BD Biosciences, San Diego) at 1:2,000. Blots were developed by using ECL Western blotting detection reagents (GE Healthcare) per manufacturer's recommendations. The ³⁵S-labeled substrates were made by using the TNT quick-coupled transcription/translation system (Promega) according to the manufacturer's recommendations and were then treated with vehicle only or with 1 μ M rGzm B at 37°C.

Fluorescent 2D DIGE. For detailed 2D DIGE and MS methods, see *Supporting Materials and Methods*, which is published as supporting

This paper was submitted directly (Track II) to the PNAS office.

Abbreviations: 2D DIGE, 2D difference gel electrophoresis; Gzm, granzyme; r, recombinant; ICAD, inhibitor of caspase-activated DNase; hnRNP, heterogeneous nuclear ribonucleoprotein; Hop, Hsp70/Hsp90 organizing protein; z-VAD-fmk, benzyloxycarbonyl-Val-Ala-Asp-fluoromethyl ketone; z-DEVD-fmk, *N*-benzyloxycarbonyl-Asp-Glu-Val-Asp fluoromethylketone; Ac-IETD-CHO, acetyl-Ile-Glu-Thr-Asp-CHO; Cy2, 3-[(4-carboxymethyl)-phenylmethyl]-3'-ethyloxycarbocyanine halide *N*-hydroxysuccinimidyl ester; Cy3, 1-(5-carboxypentyl)-1'-propylindocarbocyanine halide *N*-hydroxysuccinimidyl ester; Cy5, 1-(5-carboxypentyl)-1'-methylindodicarbocyanine halide *N*-hydroxysuccinimidyl ester.

*To whom correspondence should be addressed at: Washington University School of Medicine, Division of Metabolism, Campus Box 8127, 660 South Euclid Avenue, St. Louis, MO 63110. E-mail: rtownsend@proteomics.wustl.edu.

§To whom correspondence should be addressed at: Washington University School of Medicine, Division of Oncology, Campus Box 8007, 660 South Euclid Avenue, St. Louis, MO 63110. E-mail: tley@im.wustl.edu.

© 2004 by The National Academy of Sciences of the USA

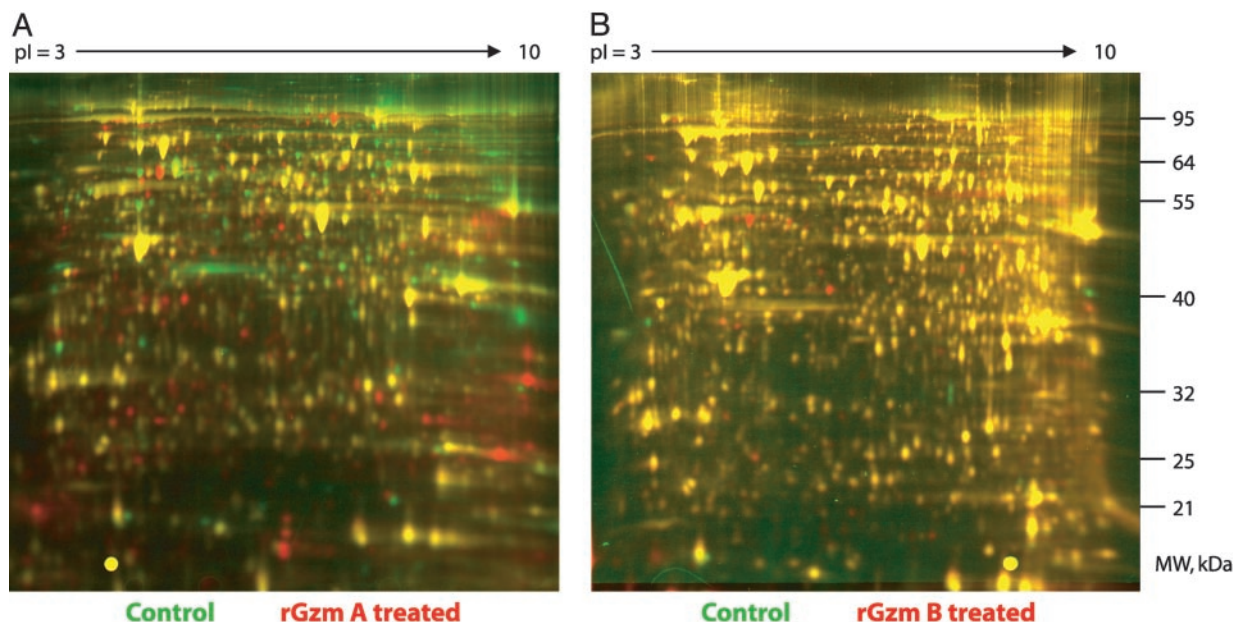


Fig. 1. Use of 2D DIGE detects multiple Gzm-mediated cleavage events. (A) YAC-1 cell freeze/thaw lysates, prepared in the presence of caspase inhibitors, were treated with $1 \mu\text{M}$ rGzm A (labeled red) or with no protease (labeled green) for 60 min at 37°C . Samples were combined and separated in two dimensions. Protein spots shared between the two samples appear yellow. Protein spots that are reduced in abundance after protease digestion (i.e., protease substrates) are green, and new spots (i.e., cleavage products) that appear after protease digestion are red. (B) Cells were lysed in the presence of caspase inhibitors, and lysates were subsequently treated with $1 \mu\text{M}$ rGzm B (red) or no protease (green) for 60 min at 37°C ($n = 3$).

information on the PNAS web site. Briefly, cells were solubilized in lysis buffer, labeled with 1-(5-carboxypentyl)-1'-propylindocarbocyanine halide *N*-hydroxysuccinimidyl ester (Cy3), 1-(5-carboxypentyl)-1'-methylindocarbocyanine halide *N*-hydroxysuccinimidyl ester (Cy5), or 3-[4-carboxymethyl]phenylmethyl-3'-ethylloxycarbocyanine halide *N*-hydroxysuccinimidyl ester (Cy2), and combined according to the experimental design. First-dimension isoelectric focusing was performed on immobilized pH gradient strips (24 cm; pH 3.0–10.0, nonlinear) in an Ettan IPGphor system (GE Healthcare). Second-dimension separation was performed on 10% isocratic SDS/PAGE gels (20×24 cm). Images were acquired on a Typhoon 9400 scanner (GE Healthcare) and relative quantification of matched gel features was performed by using Decyder DIA and BVA software (GE Healthcare).

In Vitro Cell Death Reconstitution Assay. YAC-1 cells were pre-treated with *z*-DEVD-fmk and *z*-VAD-fmk ($100 \mu\text{M}$ each) or DMSO for 30 min, and were then treated with $2 \mu\text{M}$ rGzm B and perforin-enriched natural killer cell extract as described (13). After a 60-min incubation at 37°C , cells were pelleted, resuspended at 10^8 cells per ml in 25 mM Tris-HCl/30 mM NaCl/1 mM DTT, pH 8.0 containing $100 \mu\text{M}$ *z*-DEVD-fmk, $100 \mu\text{M}$ *z*-VAD-fmk, and $200 \mu\text{M}$ Ac-IETD-CHO, and were lysed by freeze/thaw as described above. For some samples treated with perforin only, rGzmB was added at $2 \mu\text{M}$ during the first freeze cycle to control for adventitious cleavage during freeze/thaw. Lysates were solubilized in 1.5 volumes of lysis buffer.

Results

Use of 2D DIGE Detects Granzyme-Induced Cleavage Events. Cytotoxic lymphocytes can deliver perforin and Gzm B (and other effector molecules) to target cells to induce apoptosis (8). Some cell lines are exquisitely sensitive to cytotoxic lymphocyte-mediated killing, including the murine target cell line (YAC-1) evaluated in this study. Purified perforin can be used to deliver rGzm B to these target cells *in vitro*, and apoptosis is rapidly induced (12). However, it is difficult to deliver large amounts of rGzm B to all target cells using this

method. To ensure uniform accessibility of rGzm B to cellular proteins, we decided to freeze/thaw YAC-1 cells to gently disrupt the plasma membrane and minimally alter native proteins. The proteins present in these extracts were treated with recombinant murine rGzm A or rGzm B, and analyzed by 2D DIGE to assess patterns of cleavage.

YAC-1 freeze/thaw lysates were treated with either $1 \mu\text{M}$ murine rGzm A (17) or with $1 \mu\text{M}$ murine rGzm B (18) for 60 min. The protease-treated lysates were then labeled with the red fluorescent dye Cy5 and the untreated lysates were labeled with the green dye Cy3. The dyes, which are mass (≈ 500 Da) and charge (+1) matched, modify lysine residues, resulting in no net change in pI (16). Paired treated and untreated samples were combined and separated on the same 2D gel. Each gel was then sequentially scanned at the excitation and emission wavelengths specific for each fluorescent label, and the images were overlaid digitally (Fig. 1). Spots present in greater abundance in the control sample appear green and indicate possible protein substrates, whereas spots present in greater abundance in the Gzm-treated sample appear red, indicating the appearance of potential cleavage products. The observed changes were not due to differences in labeling efficiency between Cy3 and Cy5, because 2D gel analyses of two separate aliquots of the same sample (one labeled with each dye) resulted in no reproducible changes (data not shown).

Approximately 200 rGzm A-induced changes were detected with this technique (Fig. 1A). In contrast, rGzm B treatment of YAC-1 lysates resulted in only ≈ 30 specific changes (Fig. 1B). These changes were highly reproducible with multiple independent analyses ($n > 6$). A stringent database search for a restricted 4-aa recognition motif of murine Gzm B, (I/V/L) (E/Q/D/M/S) X D (M. Garcia-Calvo, personal communication), revealed that $\approx 40\%$ of murine proteins contain at least one such motif. Because $\approx 2,500$ protein spots were resolved in the analysis shown in Fig. 1B, $\approx 1,000$ proteins would be expected to contain at least one murine GzmB recognition motif. The very small number of cleavage events detected strongly suggests that Gzm B substrate specificity depends on interactions with distinct features of the folded protein sub-

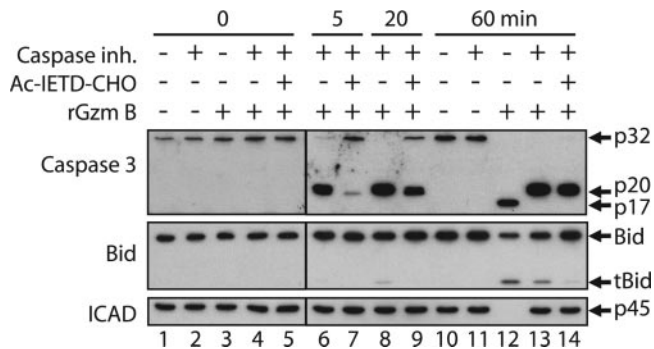


Fig. 2. Cleavage of known GzmB substrates in rGzm B-treated lysates. YAC-1 cell lysates were treated with rGzm B under different inhibitory conditions and were analyzed by Western blotting of 1D gels. The inhibitor of caspase-3 like activity, z-DEVD-fmk, and the broad-spectrum caspase inhibitor, z-VAD-fmk (100 μ M each), or vehicle control were added to YAC-1 cells before freeze/thaw-induced lysis. In the samples indicated, rGzm B was preincubated with 200 μ M Ac-IETD-CHO, a reversible inhibitor of Gzm B. The samples in lanes 11 and 13 correspond to the control and rGzm B-treated samples, respectively, shown in Fig. 1B. Similar analyses were performed at least four times with the same results.

strates. Importantly, the changes induced by Gzms A and B were completely distinct, except for one substrate spot that changed with both enzymes. The identity of this protein could not be ascertained by MS (see below).

Because Gzm B induced many fewer changes than Gzm A, we decided to first characterize this limited set of potential substrates. In addition, because a peptide-based inhibitor of Gzm B is available, we were able to evaluate the Gzm B specificity of these cleavage events experimentally.

Several proteases with known apoptotic functions are activated by Gzm B cleavage, including procaspase-3 and procaspase-8, among others (8). To identify Gzm B-specific substrates, it was necessary to prevent Gzm B-activated caspases from cleaving their substrates. We therefore used the caspase inhibitors z-VAD-fmk and z-DEVD-fmk to block the activities of caspases in all assays, as indicated. We have shown (13) that these inhibitors do not affect the activity of Gzm B at the concentrations used in this study. To evaluate the efficiency of the caspase blockade, we performed Western blot analyses (Fig. 2) of rGzm B-treated cell lysates (prepared identically to that shown in Fig. 1B). Caspase-3 activation was arrested at the p20 form in the presence of the caspase inhibitors, indicating that autocatalytic processing to the p17 form was blocked (ref. 19 and Fig. 2 *Top*, compare lanes 12 and 13). The processing of ICAD (20), an important substrate of caspases-3 and -7 (21), was also completely blocked (*Bottom*). Additionally, samples treated in the absence of caspase inhibitors were examined by 2D gel electrophoresis and exhibited several additional changes that were probably due to the actions of activated caspases on their substrates (Fig. 6, which is published as supporting information on the PNAS web site). Finally, the addition of a reversible inhibitor of Gzm B that reduces the cleavage of a colorimetric Gzm B substrate 5- to 10-fold (data not shown) delayed the processing of many of the protein spots (see below), demonstrating the dependence of these changes on Gzm B catalytic activity.

Multiple 2D gel analyses were performed to assess the reproducibility of rGzm B-induced changes. Spots that exhibited high reproducibility and >2-fold changes in abundance upon rGzm B treatment were excised from one or more gels (Fig. 7, which is published as supporting information on the PNAS web site), digested with trypsin, and identified by tandem MS. Table 1 summarizes the proteins that were identified from two or more gels. Procaspase-3, structural proteins, RNA-associated proteins, and a protein involved in chaperone systems were among the substrates

Table 1. Summary of Gzm B-induced changes identified by 2D DIGE and MS

Spot no.	Protein ID	Change	No. of IDs	NCBI locus ID no.
1	Procaspase-3	Decrease	2	12367
2	Hop	Increase	3	20867
3	Hop	Increase	3	20867
4	α -tubulin	Increase	5	22142
5	α -tubulin	Increase	2	22142
6	β -actin	Increase	5	11461
7	β -actin	Increase	3	11461
8	hnRNP K	Increase	2	15387
9	hnRNP A3	Decrease	2	229279
10	hnRNP A3	Increase	1	229279
11	Calreticulin	Increase	2	12317
12	Calreticulin	Decrease	1	12317
13	Caprin-1	Increase	2	53872

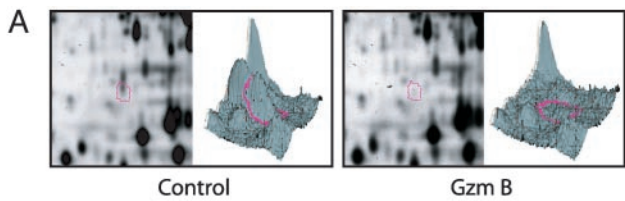
Spot numbers correspond to the numbered gel image (Fig. 8). Change, whether the spot abundance increased or decreased upon rGzm B treatment; No. of IDs, the number of independent gels from which the spot was picked and identified as the protein named. NCBI, National Center for Biotechnology Information.

identified, along with other proteins of less well defined function. These proteins all contain one or more Gzm B recognition motifs (Table 2, which is published as supporting information on the PNAS web site). Seven spots that consistently changed with rGzm B treatment could not be identified definitively, either because they were insufficiently abundant, or because the tandem spectra could not be matched to a peptide sequence in the database.

Time and Gzm B Dependence of Procaspase-3 Cleavage Observed by 2D Gel Multiplexing. The well established Gzm B substrate procaspase-3 was among the substrates identified, demonstrating that this technique can detect physiologically relevant protease substrates (19, 22–24). Fig. 3A shows gel images and 3D representations from control and rGzm B-treated samples of the spot identified as procaspase-3. The spot clearly decreases in abundance with rGzm B treatment. The peptide sequences used to identify procaspase-3 from one gel are presented in Fig. 3B. The sequences in the black boxes were identified by tandem MS and the orange shaded sequences were deduced from observed masses in the peptide pools.

To examine the time- and GzmB dependence of cleavage events, we used 2D gel multiplexing to compare multiple samples in internally controlled experiments. YAC-1 freeze/thaw lysates were treated for 0, 5, 20, or 60 min with rGzm B, or with rGzm B that had been preincubated with the reversible Gzm B inhibitor Ac-IETD-CHO. A pair of samples, one labeled with Cy3 and one with Cy5, was run on each gel. In addition, an internal standard was labeled with Cy2 and included on each gel in the experiment, allowing accurate spot matching and fluorescence quantitation among gels (25). The relative abundance of the procaspase-3 spot was then assessed across the conditions tested (Fig. 3C). In agreement with the Western blot analysis shown in Fig. 2, the processing of procaspase-3 was rapid and nearly complete within 5 min. In the presence of the Gzm B inhibitor, processing was delayed, so that complete loss of the protein spot was observed only in the 60-min sample (also see processing of the procaspase-3 p32 band in Fig. 2). An adjacent protein spot, visible in Fig. 3A directly above the spot identified as procaspase-3, changed reproducibly with similar kinetics to procaspase-3 but was not definitively identified by MS.

The Hsp70/Hsp90 organizing protein (Hop) Is a Substrate of Gzm B. We next assessed the cleavage of a previously unidentified Gzm B substrate, Hop. Hop is a cochaperone for Hsp70 and Hsp90



B

```

1  MENNKTSVDS KSIINNFVKI IHGSKSVDSG IYLDSSYKMD YPEMGIICII
51  NNNFHKSTG MSSSGTDVD AANLRFETFMG LKYQVRNKND LTFEDILELM
101 DSVSLEDHDK RSSFVCVILS HGDEGVIIYGT NGPVELKLT SFFRGDYCRS
151 LTGKPKLFI OACRSTELDC GIETDSCGDE EMACQKIPVE ADFLYAYSTA
201 PGYYSWRNSK DGSWFIQSLC SMLKLYAHKL EFMHILTRVN RKVATEFESF
251 SLDSTFHAKK QIPICVSMILT KELYFYH

```

Spot 1

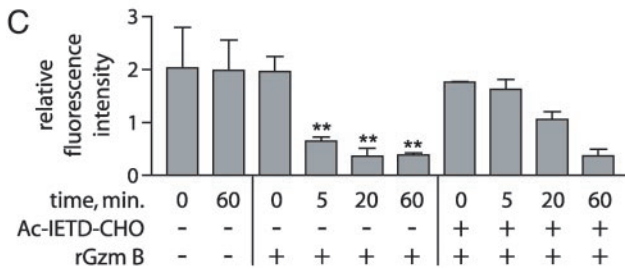
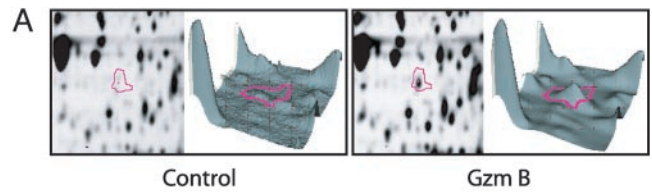


Fig. 3. GzmB-induced cleavage of procaspase-3 detected by 2D DIGE. (A) Representative gel images and 3D representations of the procaspase-3 spot ($n \geq 5$). (B) Sequence identified by tandem MS (black boxes) and sequence coverage deduced from accurate masses (orange shading) from one analysis. The red box indicates the known Gzm B recognition motif, with cleavage after the aspartic acid. D, Spot numbers correspond to the numbered gel image (Fig. 8). (C) Quantitation of spot abundance with varied cleavage conditions by using 2D gel multiplexing. Note that the addition of the reversible Gzm B inhibitor Ac-IETD-CHO slows the processing of procaspase-3. **, $P < 0.01$ vs. $t = 0$ sample ($n = 2$).

proteins (26) and has been implicated as a prion protein receptor that is involved in protecting cells from apoptosis (27). Two cleavage products of Hop were detected in our screen. Gel images showing the appearance of one of these cleavage products (spot 2) is presented in Fig. 4A. (For a numbered gel image, see Fig. 8, which is published as supporting information on the PNAS web site). Sequences identified by tandem MS and mass coverage of the two spots revealed that spot 2 contained the C-terminal cleavage fragment and spot 3 the N-terminal fragment of Hop (Fig. 4B). Importantly, one identified peptide (LGSMDEEEEAATPPPPP-PPK) derived from spot 2 was apparently generated by cleavage after D186. The accurate mass (within 20 ppm) of this peptide was detected in two independent analyses. Cleavage after an aspartic acid residue is consistent with Gzm B enzymatic activity, and the sequence surrounding this residue, LGVD ↓ LG, is in agreement with known requirements for Gzm B substrate recognition (M. Garcia-Calvo, personal communication, and refs. 5 and 6). Furthermore, one analysis (data not shown) of spot 3 detected the peptide N-terminal to this cleavage site, VMTTSLVLLGVD.

We measured the kinetics of Hop cleavage by quantifying the abundance of Hop spot 2 over the 60-min time course, using 2D gel multiplexing with an internal standard (ref. 25 and Fig. 4C). This cleavage product of Hop accumulated as a function of time, but did not appear in a control incubated for 60 min in the absence of rGzm B. The addition of the Gzm B inhibitor delayed accumulation. Similar time- and Gzm B dependence was observed for the accumulation of Hop spot 3 (data not shown).

To verify that Hop was a direct substrate of Gzm B, rather than being the substrate of a secondary protease present in YAC-1 cell lysates, we treated *in vitro*-transcribed and -translated Hop with 1



B

```

1  MEQVNELKEK GNRALSAGNI DDALQCYSEA IKLDPONHVL YSNHSAAYAK
50  KGDYQKAYED GCKTVDLKPQ WKGYSRKA ALEFLNRFEE AKRTEYEGLEK
100 HEANNVQLKE GLQNMEARLA ERKFMNPFNL PNLYQKLEND PRTRSLSDP
150 TYRELIEQLQ NKPSDLGTL QDPRVMTTLS VILGVDLGSM DEEEEAATPP
200 PPPPPKPK PEPMEEDLPE NKKQALKEKE LGNDAYKKKD FDKALKHYDR
250 AKELDPTNMT YITNQAAVHF EKGDNKCRE LCEKAIEVGR ENREDYRQIA
300 KAYARIGNSY FKEEKYKDAI HFYKNSLAEH RTPDVLKRCQ QAEKILKEQF
350 RLAYINPDLA LEEKNKGNEC FQRGDYPQAM KHYTEAIKRN PRDAKLYSNR
400 AACYTKLEF QLALKDCEEC IQLEPTFIG YTRKAAALEA MKDYTKAMDV
450 YQKALDLSS CKEAADGYQR CMAQYNRHD SPEDVKKRAM ADPEVQQIMS
500 DPAMRLILEQ MQRDPOALSE HLNPNVIAQK IQKLMVDGLT ATR

```

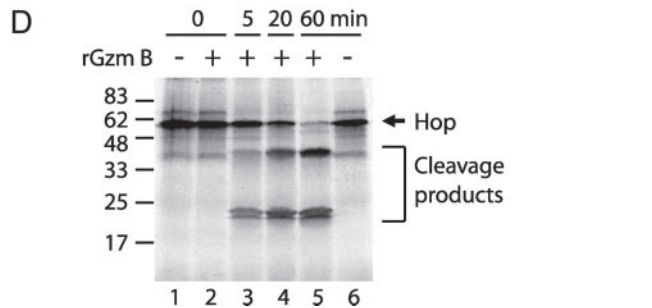
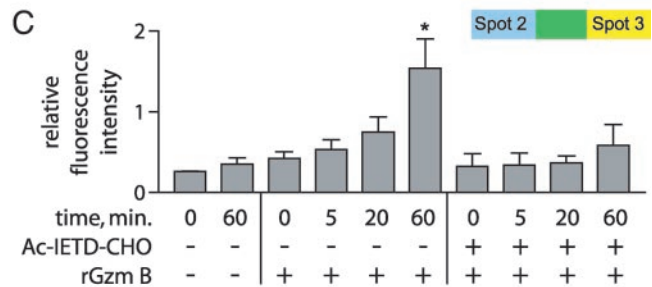


Fig. 4. Hop is cleaved by GzmB. (A) Representative gel images and 3D representations of one Hop cleavage product, spot 2 ($n \geq 5$). (B) Identified sequence and sequence coverage from one analysis, as described for Fig. 3B. Yellow and blue shaded text represent sequence coverage for two separate cleavage products of Hop that were identified ($n = 3$). The red box indicates the proposed Gzm B recognition motif. (C) Abundance of Hop with various cleavage conditions, as in Fig. 3C. Note that the addition of the Gzm B inhibitor slows the generation of the cleavage product. *, $P < 0.05$ vs. $t = 0$ sample ($n = 2$). (D) Hop was transcribed and translated *in vitro* in the presence of [³⁵S]methionine and treated with 1 μ M rGzm B at 37°C for the times indicated ($n = 5$).

μ M rGzm B for 60 min (Fig. 4D). Whereas untreated Hop remained intact (lane 6), rGzm B treatment resulted in the generation of one fragment of ≈ 40 kDa and one or two fragments of 20–25 kDa (lanes 3–5), which is in agreement with the predicted molecular weights of the cleavage products shown in Fig. 4B. A D186E mutation of Hop severely attenuated cleavage by rGzm B in this assay, proving that this is indeed the cleavage site (data not shown). Taken together, these data provide evidence that Hop is a direct substrate of Gzm B, and that it is cleaved after D186.

Cleavage of Substrates in Cells Undergoing Apoptosis Induced by Gzm B. To assess whether substrates were also cleaved in intact cells undergoing cell death induced by Gzm B, we used an *in vitro* cell death assay in which perforin is used to deliver Gzm B to target cells

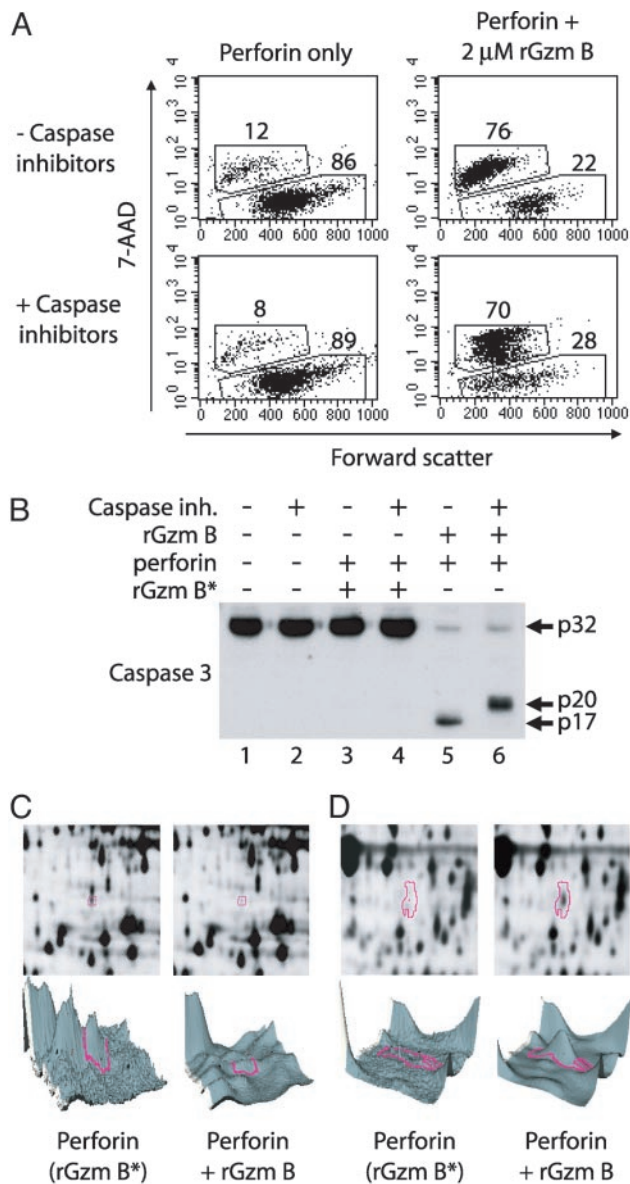


Fig. 5. Procaspase-3 and Hop are cleaved in cells undergoing GzmB-induced apoptosis. YAC-1 cells were preincubated with caspase inhibitors or vehicle control and then incubated with 2 μ M rGzm B and partially purified murine perforin for 60 min at 37°C ($n = 3$). (A) Flow cytometric analysis of 7-AAD-stained cells 60 min after treatment. The percentage of cells in each region is indicated. Note the new population of 7-AAD^{hi}/forward scatter^{lo} cells after treatment with rGzm B and perforin, indicating cell death. (B) Western blot analysis of freeze/thaw lysates from treated cells. Note that procaspase-3 is cleaved, and that its cleavage is arrested at the p20 form in the presence of caspase inhibitors (lane 6). rGzm B*, 2 μ M rGzm B was added directly preceding freeze/thaw lysis to control for protein accessibility to GzmB that occurs during preparation of the lysates. (C and D) The 2D gel images and 3D representations of procaspase-3 (C) and a Hop fragment (D) in lysates derived from treated cells preincubated with caspase inhibitors. The samples in lanes 4 and 6 from B correspond to the perforin (rGzm B*) and perforin plus rGzm B samples, respectively, in C and D.

(13). YAC-1 cells were incubated in the presence or absence of sublytic amounts of partially purified perforin and 2 μ M rGzm B. Approximately 70% of YAC-1 cells had undergone apoptosis (7-AAD^{hi}/forward scatter^{lo}) by 60 min with or without caspase inhibitor pretreatment (Fig. 5A). Freeze/thaw lysates of these treated cells were analyzed by Western blotting (Fig. 5B). Cleavage

of full-length procaspase-3 was not observed in cells treated with perforin alone, but was nearly complete in cells treated with both perforin and rGzm B. Caspase inhibition blocked generation of the autoactivated p17 form of caspase-3, as expected (28).

Proteins derived from these dying YAC-1 cells (caspase inhibitor-pretreated) were then assessed by 2D DIGE. As expected, the processing of procaspase-3 was nearly complete in 60 min (Fig. 5C). We then examined the gel for the two Hop cleavage products described above, and found both fragments in the perforin/rGzm B-treated sample, but not in the sample treated with perforin alone (Fig. 5D and data not shown). These cleavage events were not caused by the exposure of cellular proteins to rGzm B during the preparation of protein extracts, because the addition of rGzm B to the perforin-only-treated samples immediately before freeze/thaw lysis (at the end of the death assay) did not cause substrate cleavage (Fig. 5B, lanes 3 and 4, and C and D). Therefore, procaspase-3 and Hop are both cleaved in a caspase-independent manner in YAC-1 cells undergoing apoptosis induced by Gzm B.

The cleavage products of heterogeneous nuclear ribonucleoprotein (hnRNP)K, α -tubulin, and β -actin were detected in apoptotic cells only when caspase inhibitors were not added (see Fig. 9, which is published as supporting information on the PNAS web site). Cleavage of the substrates hnRNP A3, calreticulin, and caprin-1 clearly occurred in rGzm B-treated lysates, but was not detected in apoptotic cells.

Discussion

In this study, we identified Gzm substrates by evaluating the cleavage pattern of a population of native cellular proteins using 2D DIGE. Recombinant Gzm B treatment of YAC-1 cell freeze/thaw lysates resulted in the detection of a limited set of Gzm B-specific cleavage events. Procaspase-3, an important substrate of Gzm B, was identified in this screen, demonstrating the capability of this system to detect relevant substrates. Several potential Gzm B substrates were also revealed, including Hop, hnRNP K, α -tubulin, and β -actin. All were cleaved in a time-dependent, Gzm B-dependent, and caspase-independent manner in cell lysates. All four of these substrates were also cleaved in YAC-1 cells undergoing apoptosis induced by rGzm B. MS data indicate that Hop is cleaved after D186, showing that this technique can also identify protease cleavage sites.

Although caspases were efficiently inhibited in our system (Fig. 2), other secondary, Gzm B-activated proteases present in YAC-1 cell lysates could potentially be responsible for some observed cleavage events. Rapid cleavage, however, suggests direct processing by Gzm B. Indeed, the cleavage products of many identified substrates, including hnRNP K, α -tubulin, and β -actin could be detected as early as 5–20 min after Gzm B addition (data not shown), equivalent to the processing kinetics of the known Gzm B substrate Bid (Fig. 2). To prove direct cleavage by Gzm B, however, it will be important to demonstrate processing of recombinant or *in vitro*-translated substrates by rGzm B, as we have shown for Hop (Fig. 5).

The precise roles of the Gzm B substrates identified in this study are not yet clear, except for that of procaspase-3, which is a well characterized proapoptotic protease. However, several of these proteins have important roles in cellular physiology that make them potentially relevant for cell survival. Hop acts as a molecular scaffold for stress-response proteins (29, 30), which in turn can protect against apoptosis (31). Its cleavage could disrupt the organization of one intrinsic antiapoptotic mechanism. hnRNP K can mediate translational silencing by binding specific 3' UTR sequences (32); its cleavage could potentially rescue translation of mRNAs that encode proteins involved in execution of the cell. Direct cleavage of α -tubulin and β -actin, which are both structural components of the cytoskeleton, support observations that Gzm B-mediated cytoplasmic and membrane damage can take place

independent of nuclear apoptotic changes (9), even in the absence of caspase activity (33).

The proteomic screening method used in this report did not detect several known substrates of Gzm B, including Bid, poly-(ADP-ribose) polymerase, nuclear mitotic apparatus protein, and the catalytic subunit of DNA-dependent protein kinase (DNA-PK_{cs}) (34). Processing of most of these substrates by murine Gzm B has not yet been demonstrated, so it is formally possible that the murine orthologues of these proteins are not substrates of Gzm B. Also, although the 2D DIGE separation technology is capable of resolving several thousand individual protein spots on a single gel, not all proteins are resolved because of extremes of size or pI, or because of gel feature overlap in some areas. Furthermore, many low-abundance proteins are presumably not detected. Some of these limitations could be addressed by enriching potential substrates before protease treatment, and/or by altering separation techniques to increase resolution (e.g., by using narrow-range pI separations or various acrylamide concentrations). Finally, some of the known substrates of Gzm B may have been detected on the gels but not identified by MS (definitive identifications were made for 13 of 20 picked spots). Improvements in the sensitivity of MS techniques and/or improved database searching algorithms should reduce identification failures in the future.

Despite the fact that hnRNP K, α -tubulin, and β -actin are cleaved in the absence of caspase activity in YAC-1 freeze/thaw lysates, cleavage is detected in perforin/Gzm-treated whole cells only if caspases are not inhibited. The reason for this discrepancy is not yet clear. Although it is possible that these substrates may be cleaved by caspases that are activated by Gzm B in the dying cells, substrates cleaved by both caspases and Gzm B are usually cleaved at distinct sites (34, 35), which should yield distinct spots by 2D DIGE. This

finding was not the case; instead, identically located cleavage products were observed. Alternatively, some intracellular substrates may not be accessible to Gzm B unless caspases can be activated. The activated caspases may release substrates from chaperones or sequestered compartments (that are also disrupted by freeze/thaw lysis), allowing them to be cleaved by Gzm B. Differential substrate accessibility between lysates and intact cells may also account for the failure to detect hnRNP A3, calreticulin, and caprin-1 cleavage in YAC-1 cells undergoing Gzm B-induced death. Also, the kinetics of cleavage in intact cells could be reduced, and/or variable perforin-mediated delivery of Gzm B to cells (see Fig. 5A) may diminish our ability to detect some cleavage events.

This study has highlighted some of the strengths and weaknesses of a proteomically based discovery method for identifying protease substrates. Whereas proteomic methods have previously been used to identify natural protease-binding partners (36, 37), this study reveals the plausibility of using natively folded proteins as a "library" of potential targets of proteases. Our results clearly establish that this approach can be used as a rapid screen for potentially relevant protease substrates, even when there is no *a priori* knowledge of the recognition specificity of the protease. Protease proteomics may therefore represent an important tool for the discovery of substrates of many proteases.

We thank Margarita Garcia-Calvo (Merck, Rahway, NJ) for sharing unpublished data and Nancy Reidelberger (Washington University) for providing editorial assistance. This work was supported by the Cancer Research Institute (New York) (to A.J.B.), National Institutes of Health Grant DK49786 (to T.J.L.), and by an institutional grant from Washington University School of Medicine and the Siteman Cancer Center to the Proteomics Center (to R.R.T.).

1. Barrett, A. J., Rawlings, N. D. and Woessner, J. F. (1998) *Handbook of Proteolytic Enzymes* (Academic, London).
2. Yousef, G. M., Kopolovic, A. D., Elliott, M. B. & Diamandis, E. P. (2003) *Biochem. Biophys. Res. Commun.* **305**, 28–36.
3. Rawlings, N. D., O'Brien, E. & Barrett, A. J. (2002) *Nucleic Acids Res.* **30**, 343–346.
4. Overall, C. M. (2001) *Methods Mol. Biol.* **151**, 79–120.
5. Thornberry, N. A., Rano, T. A., Peterson, E. P., Rasper, D. M., Timkey, T., Garcia-Calvo, M., Houtzager, V. M., Nordstrom, P. A., Roy, S., Vaillancourt, J. P., et al. (1997) *J. Biol. Chem.* **272**, 17907–17911.
6. Harris, J. L., Peterson, E. P., Hudig, D., Thornberry, N. A. & Craik, C. S. (1998) *J. Biol. Chem.* **273**, 27364–27373.
7. Lopez-Otin, C. & Overall, C. M. (2002) *Nat. Rev. Mol. Cell Biol.* **3**, 509–519.
8. Russell, J. H. & Ley, T. J. (2002) *Annu. Rev. Immunol.* **20**, 323–370.
9. Nakajima, H., Golstein, P. & Henkart, P. A. (1995) *J. Exp. Med.* **181**, 1905–1909.
10. Goping, I. S., Barry, M., Liston, P., Sawchuk, T., Constantinescu, G., Michalak, K. M., Shostak, I., Roberts, D. L., Hunter, A. M., Korneluk, R. & Bleackley, R. C. (2003) *Immunity* **18**, 355–365.
11. Sutton, V. R., Wowk, M. E., Cancilla, M. & Trapani, J. A. (2003) *Immunity* **18**, 319–329.
12. Thomas, D. A., Scorrano, L., Putcha, G. V., Korsmeyer, S. J. & Ley, T. J. (2001) *Proc. Natl. Acad. Sci. USA* **98**, 14985–14990.
13. Thomas, D. A., Du, C., Xu, M., Wang, X. & Ley, T. J. (2000) *Immunity* **12**, 621–632.
14. Sharif-Askari, E., Alam, A., Rheaume, E., Beresford, P. J., Scotto, C., Sharma, K., Lee, D., DeWolf, W. E., Nuttall, M. E., Lieberman, J. & Sekaly, R. P. (2001) *EMBO J.* **20**, 3101–3113.
15. Unlu, M., Morgan, M. E. & Minden, J. S. (1997) *Electrophoresis* **18**, 2071–2077.
16. Tonge, R., Shaw, J., Middleton, B., Rowlinson, R., Rayner, S., Young, J., Pognan, F., Hawkins, E., Currie, I. & Davison, M. (2001) *Proteomics* **1**, 377–396.
17. Shresta, S., Graubert, T. A., Thomas, D. A., Raptis, S. Z. & Ley, T. J. (1999) *Immunity* **10**, 595–605.
18. Pham, C. T., Thomas, D. A., Mercer, J. D. & Ley, T. J. (1998) *J. Biol. Chem.* **273**, 1629–1633.
19. Martin, S. J., Amarante-Mendes, G. P., Shi, L., Chuang, T. H., Casiano, C. A., O'Brien, G. A., Fitzgerald, P., Tan, E. M., Bokoch, G. M., Greenberg, A. H. & Green, D. R. (1996) *EMBO J.* **15**, 2407–2416.
20. Liu, X., Zou, H., Slaughter, C. & Wang, X. (1997) *Cell* **89**, 175–184.
21. Wolf, B. B., Schuler, M., Echeverri, F. & Green, D. R. (1999) *J. Biol. Chem.* **274**, 30651–30656.
22. Darmon, A. J., Nicholson, D. W. & Bleackley, R. C. (1995) *Nature* **377**, 446–448.
23. Darmon, A. J., Ley, T. J., Nicholson, D. W. & Bleackley, R. C. (1996) *J. Biol. Chem.* **271**, 21709–21712.
24. Quan, L. T., Tewari, M., O'Rourke, K., Dixit, V., Snipas, S. J., Poirier, G. G., Ray, C., Pickup, D. J. & Salvesen, G. S. (1996) *Proc. Natl. Acad. Sci. USA* **93**, 1972–1976.
25. Alban, A., David, S. O., Bjorksten, L., Andersson, C., Sloge, E., Lewis, S. & Currie, I. (2003) *Proteomics* **3**, 36–44.
26. Smith, D. F., Sullivan, W. P., Marion, T. N., Zaitso, K., Madden, B., McCormick, D. J. & Toft, D. O. (1993) *Mol. Cell. Biol.* **13**, 869–876.
27. Zanata, S. M., Lopes, M. H., Mercadante, A. F., Hajj, G. N., Chiarini, L. B., Nomizo, R., Freitas, A. R., Cabral, A. L., Lee, K. S., Juliano, M. A., et al. (2002) *EMBO J.* **21**, 3307–3316.
28. Atkinson, E. A., Barry, M., Darmon, A. J., Shostak, I., Turner, P. C., Moyer, R. W. & Bleackley, R. C. (1998) *J. Biol. Chem.* **273**, 21261–21266.
29. Chen, S. & Smith, D. F. (1998) *J. Biol. Chem.* **273**, 35194–35200.
30. Lassel, M., Blatch, G. L., Kundra, V., Takatori, T. & Zetter, B. R. (1997) *J. Biol. Chem.* **272**, 1876–1884.
31. Takayama, S., Reed, J. C. & Homma, S. (2003) *Oncogene* **22**, 9041–9047.
32. Ostareck, D. H., Ostareck-Lederer, A., Wilm, M., Thiele, B. J., Mann, M. & Hentze, M. W. (1997) *Cell* **89**, 597–606.
33. Trapani, J. A., Jans, D. A., Jans, P. J., Smyth, M. J., Browne, K. A. & Sutton, V. R. (1998) *J. Biol. Chem.* **273**, 27934–27938.
34. Andrade, F., Roy, S., Nicholson, D., Thornberry, N., Rosen, A. & Casciola-Rosen, L. (1998) *Immunity* **8**, 451–460.
35. Barry, M., Heibein, J. A., Pinkoski, M. J., Lee, S. F., Moyer, R. W., Green, D. R. & Bleackley, R. C. (2000) *Mol. Cell. Biol.* **20**, 3781–3794.
36. Flynn, J. M., Neher, S. B., Kim, Y. I., Sauer, R. T. & Baker, T. A. (2003) *Mol. Cell* **11**, 671–683.
37. Fan, Z., Beresford, P. J., Oh, D. Y., Zhang, D. & Lieberman, J. (2003) *Cell* **112**, 659–672.